Incorporation of water vapor transfer in the JULES Land Surface Model: implications for key soil variables and land surface fluxes

R. Garcia Gonzalez, A. Verhoef, P. Luigi Vidale, Isabelle Braud

Incorporation of water vapor transfer in the JULES land surface model: Implications for key soil variables and land surface fluxes

Raquel Garcia Gonzalez,[1,2] Anne Verhoef,[1,2] Pier Luigi Vidale,[2,3] and Isabelle Braud[4]

Received 31 December 2011; revised 29 March 2012; accepted 9 April 2012; published 25 May 2012.

[1] This study focuses on the mechanisms underlying water and heat transfer in upper soil layers, and their effects on soil physical prognostic variables and the individual components of the energy balance. The skill of the JULES (Joint UK Environment Simulator) land surface model (LSM) to simulate key soil variables, such as soil moisture content and surface temperature, and fluxes such as evaporation, is investigated. The Richards equation for soil water transfer, as used in most LSMs, was updated by incorporating isothermal and thermal water vapor transfer. The model was tested for three sites representative of semiarid and temperate arid climates: the Jornada site (New Mexico, USA), Griffith site (Australia), and Audubon site (Arizona, USA). Water vapor flux was found to contribute significantly to the water and heat transfer in the upper soil layers. This was mainly due to isothermal vapor diffusion; thermal vapor flux also played a role at the Jornada site just after rainfall events. Inclusion of water vapor flux had an effect on the diurnal evolution of evaporation, soil moisture content, and surface temperature. The incorporation of additional processes, such as water vapor flux among others, into LSMs may improve the coupling between the upper soil layers and the atmosphere, which in turn could increase the reliability of weather and climate predictions.

Citation: Garcia Gonzalez, R., A. Verhoef, P. Luigi Vidale, and I. Braud (2012), Incorporation of water vapor transfer in the JULES land surface model: Implications for key soil variables and land surface fluxes, *Water Resour. Res.*, *48*, W05538, doi:10.1029/2011WR011811.

1. Introduction

[2] Land surface models (LSMs) simulate terrestrial energy, water, and carbon budgets based on vegetation and soil processes, in response to meteorological driving variables [*Cox et al.*, 1998, 1999]. Model-data intercomparisons may help to better understand the limitations of the measured data, the possible source of error in individual models, and the reason for the variation among model simulations [*Jung et al.*, 2007]. However, more efforts are needed not only to validate models, but also to understand the reasons of the considerable discrepancies found between models and experimental data; differences in process representation and more so, missing processes, should be considered.

[3] The transport of water and heat play a key role in the water balance and in the energy balance of terrestrial environments [*Ten Berge*, 1990; *Bitelli et al.*, 2008]. For correct predictions of soil water and heat flow by LSMs, in particular in the first few centimeters of the near-surface soil profile, we have to consider in detail all the relevant physical processes involved [*Milly*, 1982]. Soil hydrology and soil thermodynamics in LSMs are coupled through soil water phase changes, latent heat transfer, and the fact that soil thermal parameters vary due to changes in soil moisture content.

[4] Often, below-groundwater vapor fluxes in LSMs are neglected and the simplified Richard's equation is used instead. However, vapor transfer may affect the energy balance fluxes (latent and sensible heat flux) simulated for hydrometeorological and climate studies [*Bittelli et al.*, 2008]. Furthermore, processes occurring in the topsoil layers may affect water and heat flux dynamics in the deeper layers [*Grifoll et al.*, 2005], as well as estimates of heterotrophic respiration and variables related to nitrogen cycling [*Zaehle et al.*, 2010b], for example, which will have important implications for long-term predictions of the climate system [*Zaehle et al.*, 2010a].

[5] The processes related to the energy balance and soil hydrology/thermodynamics in LSMs may contribute considerably to variation among model simulations. Some models are poor predictors of key soil water balance components, due to the fact that certain processes are neglected (such as vapor transfer), or as a result of assumptions made about the accessibility of water in deeper soil layers by tree roots, in particular during periods of water deficit, or due to the way runoff and drainage are represented [*Stockli et al.*, 2007]. Other possible sources of uncertainty are related mainly to the way canopy structure, light interception, photosynthetic capacity, and the formulation of stomatal conductance, as well as the effect of soil water stress on canopy exchange, are simulated [*Jung et al.*, 2007; *Egea et al.*, 2011].

[1]Department of Geography and Environmental Science, University of Reading, UK.
[2]Walker Institute, University of Reading, Reading, UK.
[3]NCAS-Climate, University of Reading, Reading, UK.
[4]Hydrology-Hydraulics Department, IRSTEA, UR HHLY, Lyon, France.

0043-1397/12/2011WR011811

[6] Another important uncertainty arises from the resolution of the upper soil layers [*Lee et al.*, 1999; *Varado et al.*, 2006]. The vertical soil resolution varies enormously between LSMs and determines, together with the initial moisture content and soil texture, the amount of soil water available and its seasonal variability, and hence may help to explain the large divergence in model response found in intercomparisons of land-atmosphere simulations [*Seneviratne et al.*, 2006]. Although previous studies have addressed the issue of vertical soil resolution in LSMs, as well as the effect of boundary condition parameterizations [*Best et al.*, 2005], most LSMs still use a rather coarse vertical soil resolution to account for the water and soil heat transfer, despite its importance in correctly simulating the moisture profiles near the soil surface [*Braud et al.*, 1995].

[7] Finally, data assimilation from remote-sensing products may improve our model predictions. An example of this is the derivation of total soil water content from surface soil water estimation in the very first centimeters of the surface using a detailed process-based LSM [*Calvet et al.*, 1998]. In this context, LSMs schemes should aim to use a detailed hydrology scheme providing an accurate representation of the processes at the time scales observed by satellite instruments, as well as an adequate framework for the implementation of forward satellite simulators.

[8] In this paper we have implemented water vapor transfer into the JULES LSM to address some of these issues. Water vapor transfer was not incorporated in previous versions of the MOSES/JULES model (Joint UK Environment Simulator [*Cox et al.*, 1999]), nor has it been implemented in other operational models in the past. JULES is currently used at the Met Office for operational weather forecasting, for seasonal prediction, as well as for the production of Hadley Centre climate projections for the next IPCC report (AR5). Existing papers on the effect of incorporation of water vapor transfer on the water and energy balance [e.g., *Milly*, 1982, 1984; *Scanlon and Milly*, 1994; *Grifoll et al.*, 2005] study its influence over relatively short time periods (a number of days) and for single sites. Here we use multiyear diurnal time series, over three different sites. We assessed the effect of the water vapor flux on the simulated soil moisture profiles and on the processes occurring at the surface, mainly in terms of evaporation rates and surface temperatures. The aim of this study was to test the relative importance of the processes involved when modeling soil heat and water flow as a coupled process, at the local (field) scale. In a follow-up study we will assess the impact of the newly incorporated water vapor flux into JULES on a global scale in the context of coupled land-atmosphere simulations at the mesoscale.

2. Methods

[9] The changes implemented in JULES relating to the incorporation of water vapor transfer were largely based on the theory presented by *Milly* [1982, 1984], as well as on the SiSPAT model (Simple Soil Plant Atmosphere Transfer model [*Braud et al.*, 1995]). SiSPAT is a one-dimensional (1-D) model which has been used at the local scale; it solves the fully coupled heat and water transfer equations in the soil-plant-atmosphere continuum. Contrary to JULES, water vapor transfer is considered in SiSPAT. Sensitivity tests using SiSPAT initially helped to quantify the changes that we expect to find when we introduce water vapor transfer in JULES.

[10] In sections 2.1 and 2.2 a brief description of the JULES soil hydrology and heat transfer equations, as well as the theory behind the incorporation of water vapor flux, will be given.

2.1. Jules Land Surface Model

[11] JULES version 2.2 (Joint UK Environment Simulator [*Cox et al.*, 1998; *Blyth et al.*, 2010; *Clark et al.*, 2011; *Best et al.*, 2011]) is a terrestrial biosphere model which consists of two major components: (a) MOSES 2 (Met Office Surface Exchange System), which simulates photosynthesis and calculates the exchanges of energy and water between the atmosphere and the land surface and (b) TRIFFID, which can simulate prescribed or dynamic vegetation. In the standard JULES configuration, the soil profile is divided into four layers (with thickness, starting at the soil surface, of 0.10, 0.25, 0.65, and 2.0 m).

[12] The flow of water through each layer in the original version of JULES can be described as

$$C_{h,i}\frac{\partial \psi_i}{\partial t} = \frac{\partial}{\partial z}\left[K_i\frac{\partial \psi_i}{\partial z} - K_i\right] - E_i, \tag{1}$$

where ψ_i is the soil matric potential (m), K_i is the hydraulic conductivity (kg m^{-2} s^{-1}), z is depth in the profile (m), t is time step (s), and $C_{h,i}$ is the capillary capacity (kg m^{-3}). E_i is the evapotranspiration (kg m^{-2} s^{-1}) with contributions of bare soil evaporation and transpiration extracted by plants in each layer. The lower boundary condition for the water flow imposes an isothermal water flux at the bottom of the soil profile (free drainage).

[13] The heat transport is solved using the heat diffusion equation; heat transfer is coupled to the soil hydrology in that it considers soil water phase changes and variability of soil thermal properties with soil moisture content [*Cox et al.*, 1998; *Best et al.*, 2011]. The temperature T_i (K) of each layer is updated due to diffusive heat fluxes (G_i, W m^{-2}) in and out of the layer and the net heat flux advected ($J_i\Delta z_i$, W m^{-2}) to or from the layer by the moisture flux:

$$C_A\Delta z_i\frac{\partial T_i}{\partial t} = G_{i-1} - G_i - J_i\Delta z_i, \tag{2}$$

where Δz_i is the thickness of each layer (m) and C_A is the apparent volumetric heat capacity of the ith layer (J m^{-3} K^{-1}) which includes the contribution of liquid water and ice, and their phase changes.

[14] JULES (MOSES 2) includes an implicit scheme, which remains numerically stable and accurate at longer time steps than previous MOSES versions. In JULES, soil moisture and soil temperature are incremented together with the other prognostic variables at the surface. The water and heat transfer equation are solved routinely using a tridiagonal set of equations by Gaussian elimination. Within the soil JULES uses a mixed form of the Richards equation, applied to prognostic increments and to the partial derivatives of the fluxes with respect to the prognostic variables (total soil moisture content and soil temperature). As reported by *Celia et al.* [1990], this mixed form of

Richards equation yields reliable and robust numerical solutions for unsaturated flow problems. The numerical implementation allows for the prognostic time step to be independent of the driving variable time step.

2.2. Incorporation of Additional Processes in JULES

[15] LSMs generally do not consider isothermal and thermal water vapor transfer, despite the fact that water vapor transfer may considerably affect the total water flux, as well as heat transfer, especially for (semi-) arid regions [*Bittelli et al.*, 2008]. *Philip and De Vries* [1957], from hereon referred to as PDV, introduced the basis of modeling coupled moisture and heat flows, which was later modified by *Milly* [1982]. This modified approach is used in the SISPAT model and we implemented it into JULES. The aim of this study is to investigate the potential value of incorporating water vapor transfer in LSMs that are used in operational mode.

[16] Now, the total flux of moisture for each soil layer (W_m, kg m^{-2} s^{-1}) is given by the sum of the liquid flux and the water vapor flux:

$$W_m = W_l + W_v = -K_i\nabla(\psi - z) - D\nabla\rho_v. \tag{3}$$

[17] Here $D\nabla\rho_v$ corresponds to the diffusion of vapor in a homogeneous porous medium, where D is the effective molecular vapor diffusivity (m^2 s^{-1}).

[18] When there is a local equilibrium between the liquid and vapor phases, the vapor density can be given as the product of the vapor density at saturation ($\rho_{v,\mathrm{sat}}$, kg m^{-3}) and the vapor relative humidity ($h_{v,r}$):

$$\rho_v(\psi, T) = \rho_{v,\mathrm{sat}} h_{v,r} = \rho_{v,\mathrm{sat}}(T) e^{\frac{\psi g}{RT}}, \tag{4}$$

where g is the acceleration of gravity (9.8 m s^{-2}), R is the gas constant for water vapor (461.5 J kg^{-1} K^{-1}), T is the absolute temperature (K), and ψ is the soil matric potential (m) of each layer.

[19] The gradient of the vapor density can be expressed in terms of the gradient of soil water matric potential and the gradient of the soil temperature; hence there will be two terms for water vapor flux in equation (3):

$$\nabla\rho_v = \frac{g\rho_v}{RT}\nabla\psi + \left(h_{v,r}\frac{\partial\rho_{v,\mathrm{sat}}}{\partial T} - \frac{g\rho_v\psi}{RT^2}\right)\nabla T. \tag{5}$$

[20] PDV did not consider the dependence of the relative humidity of the soil air on soil temperature. However, it was noticed that local microscopic temperature gradients could be much larger than macroscopic temperature gradients. Therefore, a correction factor was introduced to take into account the enhancement factor (ξ) for vapor flux under the influence of a temperature gradient [*Cass et al.*, 1984; *Ho and Webb*, 1999; *Lu et al.*, 2011]. Scientific views on the theory behind enhancement factors vary and some authors suggest that enhancement factors are not needed if a proper capillary transport theory is employed, incorporating soil pore geometry and connectivity effects (see *Shokri et al.* [2009] and *Grifoll et al.* [2005] for further information). Unfortunately, results in this area are not conclusive and the enhancement factors approach is still widely used in soil-vegetation-atmosphere transfer schemes (SVATs) [*Saito et al.*, 2006; *Braud et al.*, 2009]. Enhancement factors seem to play a more important role for dry soil with low relative saturation (E. Shahraeeni, personal communication, 2011). Recent modeling studies have been conducted to estimate the vapor enhancement factor by matching theory with measurements. *Lu et al.* [2011] published a study where they estimated the water vapor enhancement factor from the apparent soil thermal conductivity. This is an indirect way to estimate enhancement factors and a step forward in incorporating reliable enhancement factors in unsaturated flow problems in the future. They found ξ values ranging between 1.0 and 15.0. In the current study the enhancement factor is used in the thermal vapor diffusion term and it is given by the equation presented by *Cass et al.* [1984]:

$$\xi = 8 + 3S_{u,i} - 7e^{10S_{u,i}^3}, \tag{6}$$

where $S_{u,i}$ ($\theta_{u,i}/\theta_{s,i}$) is unfrozen soil moisture content for each layer (in m^3 H$_2$O m^{-3} soil) as a fraction of liquid soil moisture content at saturation ($\theta_{s,i}$ in m^3 H$_2$O m^{-3} soil).

[21] This model delivers ξ values ranging between 1 and 10, which corresponds well with the experimental values derived by *Lu et al.* [2011].

[22] Based on the above, the total flux of moisture can be reformulated as

$$W_m = -\left(K_i + \frac{gD_a\rho_v}{RT}\right)\nabla\psi - D_a\xi\left(h_{v,r}\frac{\partial\rho_{v,\mathrm{sat}}}{\partial T} - \frac{g\rho_v\psi}{RT^2}\right)\nabla T + K_i. \tag{7}$$

[23] Finally, the conservation of water mass, considering liquid water as well as water in the form of vapor, per unit volume of soil is given by

$$\frac{\partial}{\partial t}\left(\rho_w\theta + \rho_v(n-\theta)\right) = -\nabla W_m = \nabla[(K_i + D_{\psi,v,i})\nabla\psi + D_{T,v,i}\nabla T - K_i] - E_i, \tag{8}$$

where ρ_w is the density of water (kg m^{-3}), n is the soil porosity (m^3 m^{-3}), ρ_v is the vapor density in the soil air (kg m^{-3}), θ is the volumetric liquid soil moisture content (m^3 m^{-3}) and $(n - \theta)$ is the volumetric soil air content (m^3 m^{-3}).

[24] The isothermal vapor conductivity for each layer ($D_{\psi,v,i}$) can be obtained with

$$D_{\psi,v,i} = \frac{D_a\Omega(n-\theta)}{\rho_w}\left.\frac{\partial\rho_v}{\partial\psi}\right|_T, \tag{9}$$

where Ω represents the tortuosity of the air-filled domain ($\Omega = (n - \theta)^{2/3}$, as by *Lai et al.* [1976]), and D_a is the molecular diffusivity of water vapor in the air (m^2 s^{-1}) [*Kimball et al.*, 1976]:

$$D_a = 2.17 \times 10^{-7}\left(\frac{T}{273.15}\right)^{1.88}. \tag{10}$$

[25] The thermal vapor diffusion coefficient ($D_{T,v,i}$) due to temperature gradients is given by (following *Milly* [1984])

$$D_{T,v,i} = \frac{D_a(n-\theta)\xi}{\rho_w}\left.\frac{\partial \rho_v}{\partial T}\right|_{\psi}. \quad (11)$$

[26] The incorporation of the isothermal and thermal water vapor transfer into the existing below-ground parameterizations of JULES affects the simplified Richard's equation, equation (1) of this paper, which was therefore reformulated as

$$C_{h,i}\frac{\partial \psi_i}{\partial t} = \frac{\partial}{\partial z}\left[(K_i + D_{\psi,v,i})\frac{\partial \psi_i}{\partial z} + D_{T,v,i}\frac{\partial T_i}{\partial z} - K_i\right] - E_i. \quad (12)$$

[27] The heat transfer equation has to be modified as well; the heat of wetting due to soil matric potential gradients has to be incorporated. Hence, equation (2) is changed as follows:

$$C_A \Delta z_i \frac{\partial T_i}{\partial t} = \frac{\partial}{\partial z}\left[\lambda_i \frac{\partial T_i}{\partial z} + \rho_w L D_{\psi,v,i}\frac{\partial \psi_i}{\partial z}\right] - c_w W_{l,i}\Delta z_i \frac{\partial T_i}{\partial z}, \quad (13)$$

where λ_i is the apparent thermal conductivity (W m^{-1} K^{-1}) of each layer; c_w is the specific heat capacity of the soil water (J kg^{-1} K^{-1}), L is the latent heat of vaporization of water (2.44 $\times$ 10^6 J kg^{-1} at 25°C) and $W_{l,i}$ is the vertical liquid water flux (kg m^{-2} s^{-1}) in the soil, given by Darcy's law. C_A has also been updated to take into account the heat capacity associated with water vapor and liquid-vapor phase changes.

[28] In summary, vertical fluxes of water can be decomposed into liquid fluxes, which are driven by water potential gradients, and vapor fluxes, which are driven by vapor pressure gradients (usually called isothermal vapor flux or convection in vapor phase) and temperature gradients (called thermal vapor flux or diffusion in vapor phase), respectively (see equations (8) and (12)).

2.3. Site Descriptions

[29] Water vapor transfer plays a more prominent role in bare or sparsely vegetated soil surfaces, in particular when these soils are located in arid or semiarid environments; vegetation modulates the mass and energy balance through root water uptake and subsequent transpiration. Hence, water vapor flux makes a relatively small contribution to the total water and heat transfer under vegetated conditions. Therefore, this study focused on sites with relatively sparse vegetation cover (and short vegetation only, i.e., grasses/herbs) to avoid confusion with vegetation-dominated processes. In addition, sensitivity runs were also performed for the Rothamsted Research site (Harpenden, UK) (Lat. 51.49N, Lon. 0.21W) situated in the south of the UK with an annual average precipitation of ~800 mm with short grass vegetation. As we expected the effect of incorporation of water vapor flux on the modeled evaporation did not play an important role for this site experiencing subhumid climatic conditions; differences were only ~4–5 W m^{-2} when latent heat values were of the order of 150 W m^{-2}. Water vapor flux will play a more important role for sites with prolonged dry spells and precipitation of ~500 mm or lower, in particular when sparsely vegetated.

[30] Model studies were performed for three sites with different climate and soil properties: the Jornada experimental range, about 40 km north of Las Cruces, New Mexico (USA); the Griffith site, which was part of the Murrumbidgee soil moisture monitoring program (Australia), and the Audubon site (Arizona, USA), part of the Ameriflux Network (http://public.ornl.gov/ameriflux/). Special care was taken to choose sites with extensive meteorological time series that exhibited different rainfall intensities and frequencies, adding climatology significance to this study, in contrast with short-term, single-site studies [*Scanlon and Milly*, 1994; *Milly*, 1982, 1984; *Grifoll et al.*, 2005].

[31] The Jornada site (Lat. 35.57N, Lon. 106.5W) has a semiarid climate characterized by a wide range of diurnal temperatures with generally low relative humidity and intense and convective storms of short duration [*Nash and Daugherty*, 1990] with an annual average precipitation of 233 mm [*Wondzell et al.*, 1990]. The soil at the Jornada site is a sandy loam. The Griffith site (Lat. 34.24S, Lon. 146.1E) belongs to the Murrumbidgee River catchment in southeast Australia with an annual average precipitation of 437 mm [*Richter et al.*, 2004]. The soil at Griffith site can be classified as loam or clay-loam. The Audubon site (Lat. 31.6N, Lon. 110.5W) is a temperate arid site with an annual average precipitation of 376 mm (generally July marks the onset of the rainy season) and a sandy loam soil [*Meyers*, 2009; *Thompson* et al., 2011]. These three sites are characterized by relatively long dry periods disrupted with intermittent rainfall events; dry spells are longer for the Jornada and Audubon site, while precipitation at the Griffith site seems to be more evenly distributed over time. We will see in section 3 that these precipitation patterns are important to understand the water dynamics and evaporation rates at these sites.

[32] Atmospheric driving variables were available for all three sites. JULES is driven by half-hourly atmospheric variables: rainfall rate, shortwave and longwave radiation, air temperature, specific humidity, and wind speed. Concerning the verification variables: soil moisture contents were only available for the Jornada and Griffith site (see section 3.1); surface temperatures and latent heat measurements were only available for the Jornada site and the Audubon site, respectively (see section 3.3). Installation heights and depths of the atmospheric and soil physical sensors used at the sites, as well as the sensors employed, are given by *Nash and Daugherty* [1990] for the Jornada site, by *Richter et al.* [2004] for the Griffith site, and by *Meyers* [2009] for the Audubon site.

2.4. Model Parameterizations

[33] JULES allows for various options to describe the functional dependence of soil matric potential, hydraulic conductivity, and thermal conductivity on soil moisture content. The *Brooks and Corey* [1964] relationships were used in our simulations to describe the soil hydraulic properties, while thermal conductivity was calculated using the Lu approach [*Lu et al.*, 2007]. A number of soil parameters are therefore required to allow simulation of the existing heat and water processes and those additional processes

that were implemented in JULES. Note that the simulations that will be presented later on are performed in the absence of parameter fitting.

[34] At the Jornada site we obtained hydraulic and thermal properties from in-situ soil texture measurements; soil hydraulic parameters were calculated from Cosby pedotransfer equations [*Cosby et al.*, 1984] (see Table 1). Soil texture and soil moisture monthly measurements were obtained from the NPP transect (G-SUMM) nearest to the LTER weather station [*Nash and Daugherty*, 1990].

[35] It is important to mention that Cosby derived quantitative expressions for the hydraulic parameters as functions of the particle size distribution using a large data set available for analysis. However, he found a relatively large parameter variance for each soil textural class. This will introduce a source of uncertainty in the parameters.

[36] Soil hydraulic parameters for the simulations at the Griffith and Audubon [*Thompson et al.*, 2011] site were obtained from previous studies [*Richter* et al., 2004; *Thompson* et al., 2011]. We assumed that these parameters do not vary with depth.

[37] Soil thermal conductivity parameters (dry thermal conductivity, saturated thermal conductivity, and dry heat capacity) were computed using the approach by *Lu et al.* [2007]; they depend on porosity and textural composition (see Table 1 for more details).

2.5. Model Protocol

[38] From previous studies presented in the literature we know that the isothermal and thermal water vapor fluxes are particularly important in the topsoil layers. Hence we focused on the upper soil layers to study the effect of incorporation of water vapor flux into JULES. The thickness of each layer was changed to roughly match the soil depth where the measurements had been taken, while aiming to stay as close as possible to the standard JULES configuration. Hence soil layer thicknesses chosen for the Jornada and the Audubon site were 0.10, 0.25, 0.65, and 2.0 m; and for the Griffith site: 0.08, 0.14, 0.46, and 2.32 m. The choice to keep the number of soil layers to four was partly due to the fact that this configuration is used in distributed mode for the operational JULES. We aim to use this distributed model for follow up studies to determine the importance of vapor flux incorporation on regional and global water and energy balances. The use of a shorter time step to allow for thinner layers would not be operationally affordable.

[39] Nonisothermal water transport close to the soil surface can be related to steep gradients of water content and temperature. This ideally requires a relatively fine grid. Therefore, we explored the impact of the model's vertical soil resolution on the simulation of within-soil physical processes (see section 3.4) to determine whether the JULES model, with vapor flow implemented, retains its mechanistic integrity under relatively coarse grids.

[40] The simulations covered 1995–1998 for the Jornada site, 2002–2006 for the Griffith site, and 2003–2005 for the Audubon site. The fractional cover of each plant functional type was prescribed: based on the site descriptions, a value of 0.6 for C3 grasses and 0.4 for bare soil was chosen for the Jornada and Audubon site; a value of 0.4 for grasses and 0.6 for bare soil at the Griffith site. Leaf area index (LAI) was prescribed for the C3 grasses with a value of 2.0. The surface has a distinct surface and canopy level for the purpose of radiative coupling between the canopy and underlying ground [*Clark et al.* 2011]. Spin-up was used for all sites: the first year of driving data served to force model spin-up, iterating up to 10 times. Equilibrium was reached generally after two or three iterations. We also set initial conditions for the soil moisture content to measured values, when available, which helped to reduce the number of spin-up iterations.

[41] The agreement between measured and modeled soil water content and latent heat fluxes can be affected by the vegetation parameterization used in JULES (for this study C3 grasses were used). For all sites, intermittent rainfall

Table 1. Soil Hydraulic and Thermal Parameters Used for the JULES Models Runs for the Jornada, Griffith and the Audubon Site[a]

Soil Depth (m)	b	Θ_s	Ψ_s	K_s	Θ_c	Θ_w	λ_{dry}	λ_{sat}	C_d
				JORNADA					
0.05	3.6	0.385	0.066	0.0173	0.147	0.058	0.294	1.746	1322781.0
0.2	3.6	0.385	0.066	0.0173	0.147	0.058	0.294	1.746	1322781.0
0.6	4.22	0.389	0.073	0.0155	0.158	0.0642	0.291	1.708	1324005.0
2.0	5.87	0.401	0.094	0.0097	0.219	0.114	0.285	1.634	1339231.0
				GRIFFITH					
0.04	6.04	0.472	0.338	0.00457	0.323	0.171	0.254	1.250	1168452.9
0.15	6.04	0.472	0.338	0.00457	0.323	0.171	0.254	1.250	1168452.9
0.45	6.04	0.472	0.338	0.00457	0.323	0.171	0.254	1.250	1168452.9
1.80	6.04	0.472	0.338	0.00457	0.323	0.171	0.254	1.250	1168452.9
				AUDUBON					
0.05	3.6	0.385	0.066	0.0173	0.147	0.058	0.294	1.746	1322781.0
0.2	3.6	0.385	0.066	0.0173	0.147	0.058	0.294	1.746	1322781.0
0.6	3.6	0.385	0.066	0.0173	0.147	0.058	0.294	1.746	1322781.0
2.0	3.6	0.385	0.066	0.0173	0.147	0.058	0.294	1.746	1322781.0

[a]Clapp-Hornberger exponent b; volumetric soil moisture concentration at saturation Θ_s ($m^3\ m^{-3}$); saturated soil water suction Ψ_s (m); hydraulic conductivity at saturation point K_s ($kg\ m^{-2}\ s^{-1}$); volumetric soil moisture concentration at critical point Θ_c, ($m^3\ m^{-3}$); and volumetric soil moisture concentration at wilting point Θ_w ($m^3\ m^{-3}$). The wilting point and critical point are assumed to correspond to soil water suctions to 1.5 and 0.033 MPa, respectively; dry thermal conductivity λ_{dry} ($W\ m^{-1}\ K^{-1}$); saturated thermal conductivity λ_{sat} ($W\ m^{-1}\ K^{-1}$); and the dry heat capacity C_d ($J\ m^{-3}\ K^{-1}$). Hydraulic parameters (b, Θ_s, Ψ_s, and K_s) were obtained using Table 4 of *Cosby et al.* [1984]. Thermal parameters (λ_{dry} and λ_{sat}) were computed using the approach by *Lu et al.* [2007].

events during the rainy season affects vegetation, which alters the soil moisture profiles via root water uptake and transpiration. The identical inclusion of (shallow-rooted) vegetation parameterization in each numerical experiment in our design has removed the influence of vegetation water uptake on fluxes and prognostic variables related to the water balance. Changes in model skill can therefore be attributed only to the incorporation of vapor fluxes into the model.

[42] Standard soil hydrology in JULES considers four layers and liquid vapor flux only; this particular configuration (4L, with L for liquid) was considered as our control simulation. Two runs were performed with JULES for each site: (1) liquid flux only (4L, standard JULES) and (2) both liquid and vapor fluxes are considered (4LV).

3. Results and Discussion

3.1. Surface Hydrology—Model Assessment

[43] Figure 1 compares measured and modeled unfrozen soil moisture content as a fraction of saturated soil moisture content between 4L and 4LV simulations for the Jornada site. Only monthly measurements were available to validate the model from the nearby NPP transect station (G-SUMM) at 0.2, 0.6, and 2.0 m, i.e., no data were available for the first layer (0.05 m depth). There is a high variability in the simulated soil moisture content of the near surface soil layer (0.05 m) due to the intense rainfall events. JULES-4LV captures more accurately the dry-down observed during the summer months at 0.2 m for 1995, 1996, and 1998 (Figure 1b), likely due to isothermal vapor transfer being significant during the drying periods. The contribution of the vapor fluxes to simulated water transfer will be explained in detail in section 3.2. Hardly any differences are observed between JULES-4L and JULES-4LV for the deeper layers for this site (at 0.6 and 2.0 m) (Figures 1c and 1d), due to the fact that isothermal and thermal water vapor flux in the deeper layers are less important than in the topsoil layers, and also because soil moisture contents are higher. Soil moisture measurements at the Jornada site carry an inherent spatial (soil moisture measurements correspond to the transect station, approximately 0.8 km away from the meteorological station) and temporal (monthly measurements) uncertainty, so their usefulness to assess our simulations is somewhat limited. This could possibly explain the differences found between the model and the measurements, in particular for 1997. Nevertheless, JULES-4LV overall appears to have improved seasonal predictions of soil moisture content.

[44] Figure 2 shows measured (half-hourly) and modeled unfrozen soil moisture content as a fraction of saturated soil moisture content for the 4L and 4LV simulations driven by meteorological conditions collected for the Griffith site. Volumetric soil moisture was measured as a layer average for the four layers at this site, 0–0.07, 0–0.3, 0.3–0.6, and 0.6–0.9 m [*Richter et al.*, 2004; *Young et al.*, 2008], which served to assess JULES performance at 0.04, 0.15, and at 0.45 m. We therefore used a moving average (10 day) for the model output in order to allow for better

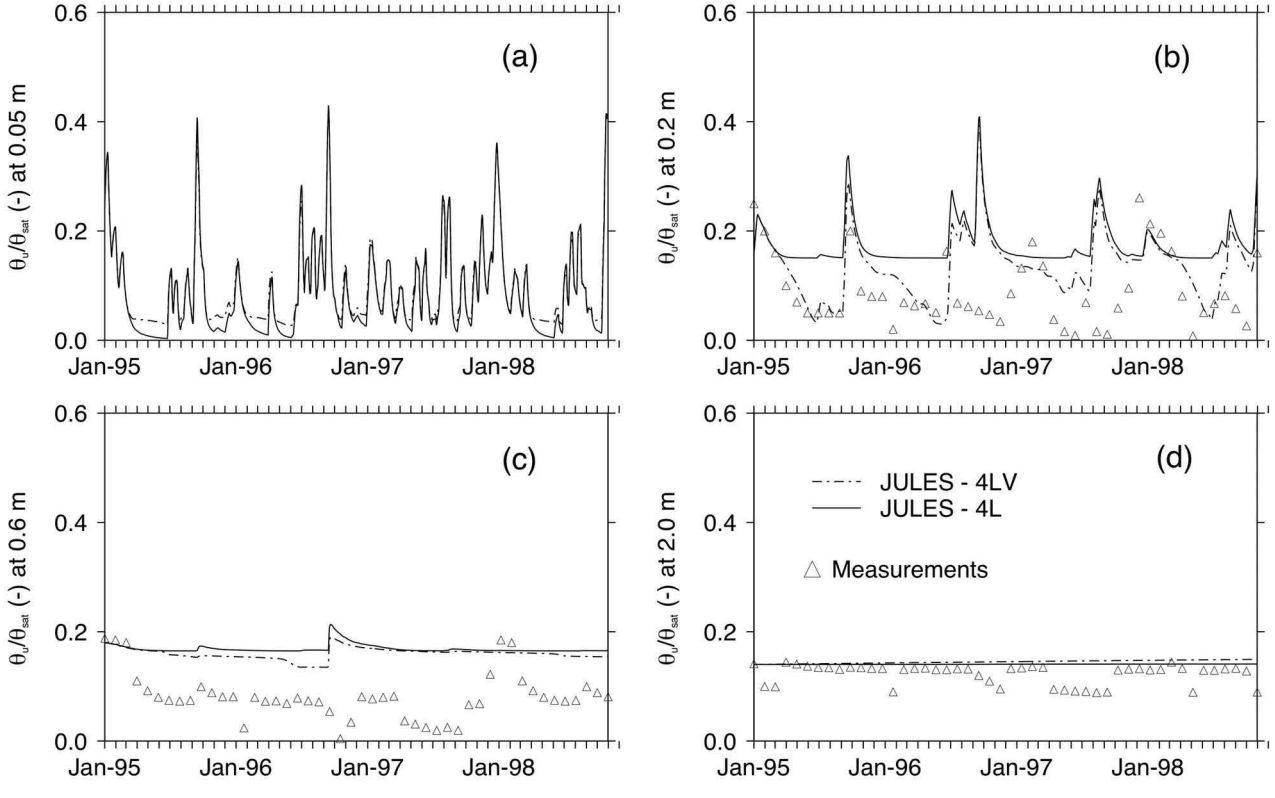

Figure 1. Measured and modeled (4L and 4LV) unfrozen soil moisture content as a fraction of saturated soil moisture content (θ_u/θ_s) at (a) 0.05 m (note, no data were available), (b) 0.2 m, (c) 0.6 m, and (d) 2.0 m for the Jornada site from 1995 to 1998.

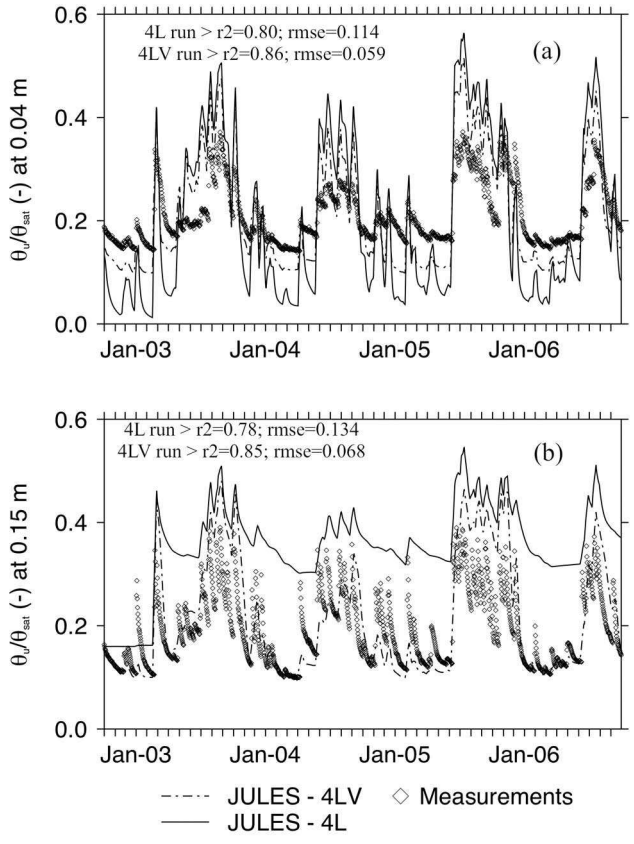

Figure 2. Measured and modeled (4L and 4LV) unfrozen soil moisture content as a fraction of saturated soil moisture content (θ_u/θ_s) at (a) 0.04 m and (b) 0.15 m for the Griffith site from October 2002 to 2007. Model performance was assessed with correlation coefficient (r^2) and root mean square error (rmse).

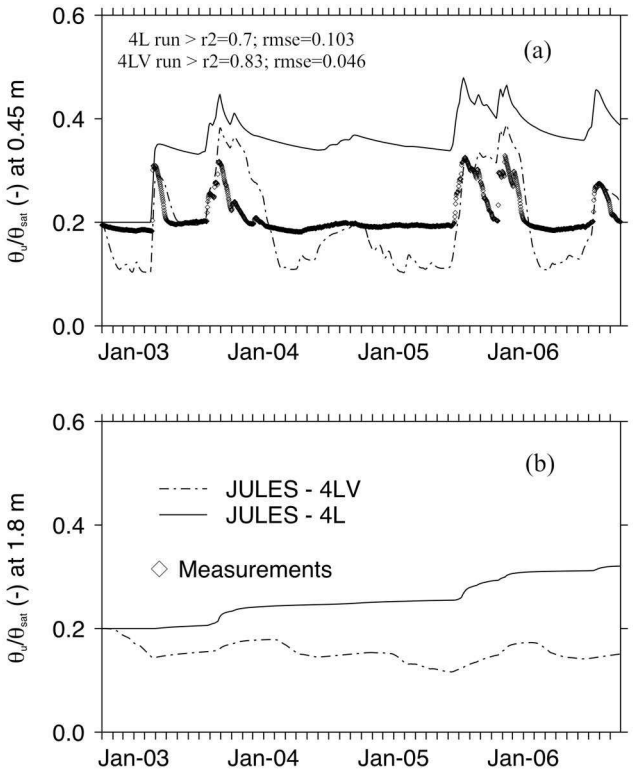

Figure 3. Measured and modeled (4L and 4LV) unfrozen soil moisture content as a fraction of saturated soil moisture content (θ_u/θ_s) at (a) 0.45 m and (b) 1.8 m (note that no measurements were available) for the Griffith site from October 2002 to 2007. Model performance was assessed with correlation coefficient (r^2) and root mean square error (rmse).

comparison with the measurements; the measured time series of layer averages were smoother than the modeled relative soil moisture contents which represented values at a particular depth, where the infiltration front would come and go very suddenly. Model performance was assessed by calculating the correlation coefficient (r^2) and root mean square error (rmse) for comparisons between modeled and measured soil moisture contents (see Figures 2 and 3). JULES-4L underestimates near-surface soil moisture content for the Griffith site, which may be explained in part by the missing water vapor flux. Similar observations have been reported in previous studies [see *Grifoll et al.*, 2005]. JULES-4LV predicts near surface soil moisture content better than the JULES-4L run, although it still underestimates θ/θ_s at 0.04 m compared to the measurements (Figure 2a). JULES-4LV captures very accurately the soil moisture content depletion at 0.15 m (Figure 2b) and its high-frequency intraseasonal dynamics. Changes in the water transfer of the topsoil layer have also modified the hydrology of the deeper layers. JULES-4L tends to overestimate soil moisture content at 0.45 m compared to JULES-4LV (Figure 3a).

[45] This section has shown that taking into account water vapor flux in the soil water budget and water transfer yields a better fit (in particular an improved evolution) between measured and modeled (relative) soil moisture content. In section 3.2 we will study the relative contribution that the isothermal and thermal vapor fluxes have to the total water transfer and how it varies with climate, soil properties, depth, and soil moisture content.

3.2. Relative Contribution of the Vapor Fluxes to Simulated Water Transfer

[46] Figure 4 shows the simulated isothermal and thermal vapor flux at 0.10 and at 0.35 m depth for the Jornada site for a period of 40 days. Thermal vapor flux becomes substantial a couple of days after the first rainfall event (30 June 1995); the drying front will develop and evaporation will decrease over time. Therefore the temperature gradient will become more pronounced and thermal vapor flux will increase.

[47] Six days after the rainfall event, the topsoil layer dries out even more and the isothermal vapor flux also starts to play a role, transferring water upward from the second layer to the topsoil layer. Between 12 and 15 July 1995 consecutive rainfall events occur which suppress the isothermal vapor flux bringing up moisture to the topsoil layer. Initially, the thermal vapor flux is again dominant, but after a few days, when the topsoil layer dries out further, isothermal vapor flux (upward) starts to build up again. A delay of approximately two days is observed, which may be related to the process of redistribution of water until

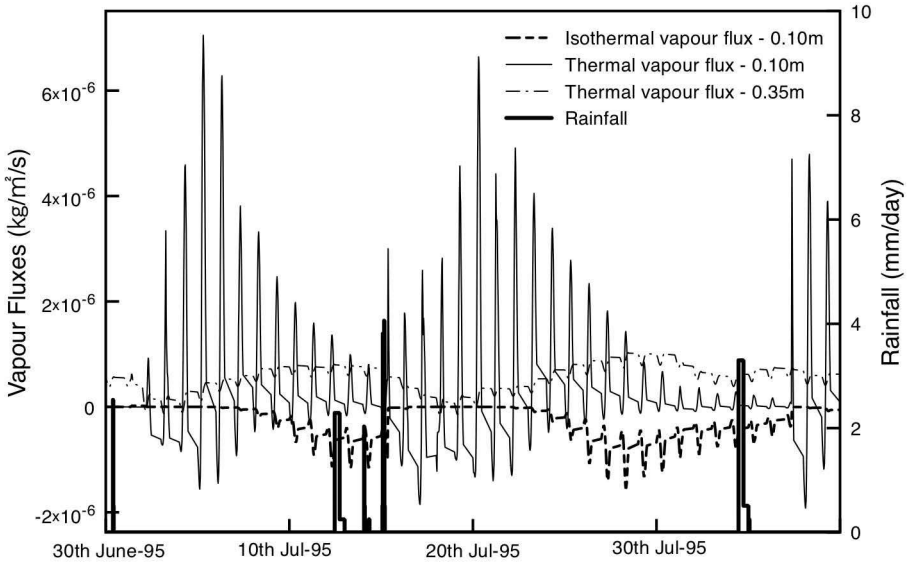

Figure 4. Simulated isothermal and thermal vapor flux (kg m^{-2} s^{-1}) at 0.10 and 0.35 m for the Jornada site (4LV simulation) between 30 June 1995 and 10 August 1995. Rainfall events are also shown. In this figure, positive fluxes are directed downward and negative fluxes are directed upward.

7 August. Figure 4 shows the water (vapor) flux dynamics of semiarid ecosystems will be different after an extended dry period compared to a period with more rainfall, but which has an intermittent pattern.

[48] The downward thermal vapor flux observed at 0.35 m (the interface between the second and third layer) (Figure 4) also contributes to the soil moisture depletion observed at 0.2 m as a result of a temperature gradient that causes a net downward thermal vapor flux. These temporal evolutions of (iso)thermal vapor fluxes illustrate that actual evaporation in arid and semiarid sites will be strongly driven by the frequency and magnitude of rainfall events. The development of the drying front after rainfall events will be important for the coupling between the land surface and the atmosphere [*Teuling et al.*, 2006], underlining the strong feedback that exists between soil moisture and precipitation in semiarid environments [*Koster and Suarez*, 2001].

[49] Temperature gradients ($\partial T_i/\partial z_i$) as the driving force for thermal vapor flux (see equation (12)) help to explain the direction of thermal vapor flux. During daytime the temperature gradient (with a larger temperature amplitude during summer than winter) between the surface and the intermediate soil layer will generate a net downward flux (dominant thermal vapor flux), which will tend to suppress soil evaporation. At night, an upward flux is observed instead due to the reversed temperature gradient between the soil surface layer and the lower soil layer.

[50] Different characteristics for the water vapor fluxes were observed for the Griffith site. Figure 5 shows the isothermal vapor flux and the simulated soil water content for the 4LV simulation at the Griffith site for the top two soil layers from November 2003 to February 2004. Isothermal vapor flux seems to play a more prominent role in this particular semiarid environment. The fact that the inclusion of water vapor transfer has a larger effect on the Griffith than on the Jornada site is partly caused by the Griffith soil containing more clay. Clay soil generally has larger values of porosity, thus also larger values of the vapor diffusion parameters [$D_{\psi,v,i}$ and $D_{T,v,I}$ are correlated to volumetric air content and tortuosity (see equations (9) and (11))].

[51] Validation of simulated in-soil water vapor fluxes with measurements is difficult, as continuous gas flow within soil is notoriously hard to measure [*Ho and Webb*, 1999; *Shahraeeni et al.*, 2010]. Some authors have used tracers of water movement, such as stable water isotopes [see *Braud et al.*, 2009]. Others have performed well-controlled laboratory experiments to simulate coupled nonisothermal multiphase flow, but they always relied on models to determine the relative role between water (liquid and vapor) flow and heat transfer [*Gran et al.*, 2011].

[52] Immediately after rainfall events, thermal vapor flux is approximately one or two orders of magnitude larger at the Jornada site. These observed patterns are due to the fact that temperature gradients are more significant for the Jornada site, because it is in general drier than the other sites. Furthermore, enhancement factors (given by equation (6)) will be more important when relative saturation is between 0.05 and 0.2 [see also *Ho and Webb*, 1999]; this is the case at the Jornada site where the enhancement factor (ξ) changes abruptly during rainfall events (taking on values between 1.0 and 10.0). By contrast, the enhancement factor at the Griffith site remains relatively constant ($\sim$2.0) due to the larger values of soil moisture content (see Figures 2a and 2b) and lower temperature gradients (as the driving force for thermal vapor fluxes) within soil layers.

[53] Figure 5 also shows that between the first and second layer there is both a liquid (positive, correlated with rainfall events; not shown in Figure 5) and vapor flux. The simulated isothermal vapor flux and the relative saturation were compared for the upper and intermediate layers in order to understand how the diffusion of water vapor affects the water transfer within layers and how this is related to the liquid water transport; an upward flux is apparent which

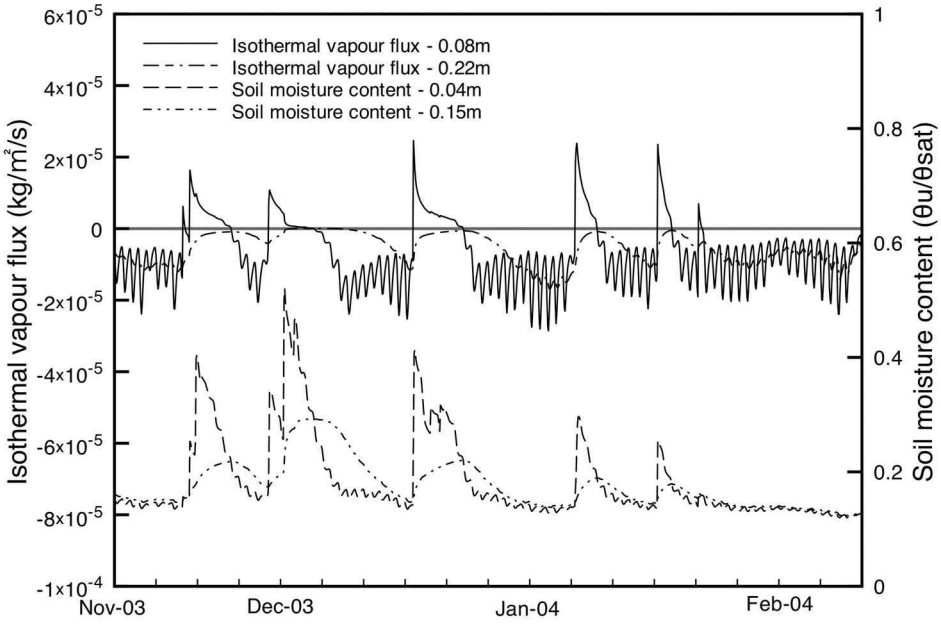

Figure 5. Isothermal vapor flux (kg m^{-2} s^{-1}) at 0.08 and at 0.22 m for the Griffith site between November 2003 and February 2004. Simulated soil moisture content as a fraction of saturated soil moisture content (θ_u/θ_s) is also shown at 0.04 and at 0.15 m. The horizontal line was included to distinguish between upward (negative) and downward (positive) isothermal vapor flux.

correlates well with a concurrent decrease of soil water content at 0.15 m. A similar evolution is found at 0.08 m, which has a diurnal nature. Soil moisture content of the upper soil layer increases at the expense of a decreased amount of water in the layer below (see Figure 2) due to the observed upward isothermal vapor flux at 0.08 m (see Figure 5). Here again, rainfall events suppress isothermal vapor flux, as was observed for the Jornada site; this flux starts to build up again after approximately six to eight days.

[54] Overall, the water vapor flux plays a significant role in the total water flux in the first 30 cm of soil at the Jornada site and in the first 20 cm at the Griffith and Audubon site (not shown). This depth, where water vapor flux is significant, is actually equivalent to the drying front as defined in previous studies [*Milly*, 1984; *Scanlon and Milly*, 1994; *Saravanapavan and Salvucci*, 2000]. Previous studies have also tried to isolate the relative contributions of liquid and vapor transport to soil evaporation [*Milly*, 1984; *Scanlon and Milly*, 1994; *Saravanapavan and Salvucci*, 2000]; they found that vapor transfer can be significant in dry conditions. Results by *Saravanapavan and Salvucci* [2000] suggested that the soil evaporation is mainly limited by the liquid water flux of the deeper and wetter soil layer below the drying front (between ~4 and 28 mm for a silty-clay soil and between 10 and 24 mm for a loamy-sand soil) where the water vapor flux is more relevant.

[55] The depth of the drying front and the magnitude of the vapor fluxes are affected by the different soil properties and meteorological variables representing the sites. Vapor transfer in the topsoil layer is found to be mainly due to isothermal vapor flux for all sites. *Milly* [1984] also found that isothermal vapor fluxes tend to be more relevant under arid or semiarid environments; thermal vapor fluxes would be also important, particularly immediately after rainfall events.

[56] Our study has shown that water vapor fluxes had a similar order of magnitude to the values found in previous studies [see for instance *Grifoll et al.*, 2005; *Gran et al.*, 2011; *Scanlon and Milly*, 1994]. Our results illustrate that vapor fluxes modify the soil hydrology, and hence the surface temperature, which impacts on the surface energy balance, in particular the evaporation flux. This will be discussed further in section 3.3.

3.3. Effect of Incorporation of Water Vapor Fluxes in JULES on the Modeled Evaporation Rates and Surface Temperatures

[57] Changes in the soil moisture contents in the root zone due to the incorporation of water vapor flux will have a direct effect on the leaf stomatal conductance (via the soil water stress parameter embedded in JULES, which depends on soil moisture content of the soil layers representing the root zone) and water uptake by plants, and hence on transpiration. In addition, the soil moisture content of the topsoil layer, and changes thereof, determines the conductance to soil evaporation. This section therefore explores the effects of these soil moisture changes on total evaporation.

[58] Figure 6a presents modeled (4L and 4LV) latent heat flux (measured rainfall amounts are also shown) for the long-term runs (between 1995 and 1998) performed for the Jornada site. Absolute differences of latent heat (Figure 6b) between the simulations 4L and 4LV are also shown. The effect of incorporation of water vapor flux in JULES on the modeled evaporation occurs via changes of water transfer in the topsoil layers, as we described in section 3.1. Water vapor fluxes do not play a significant role during winter and early spring, but their influence was important from April to approximately October of each year (onset of the rainy season at this site) via their effect on the soil moisture content

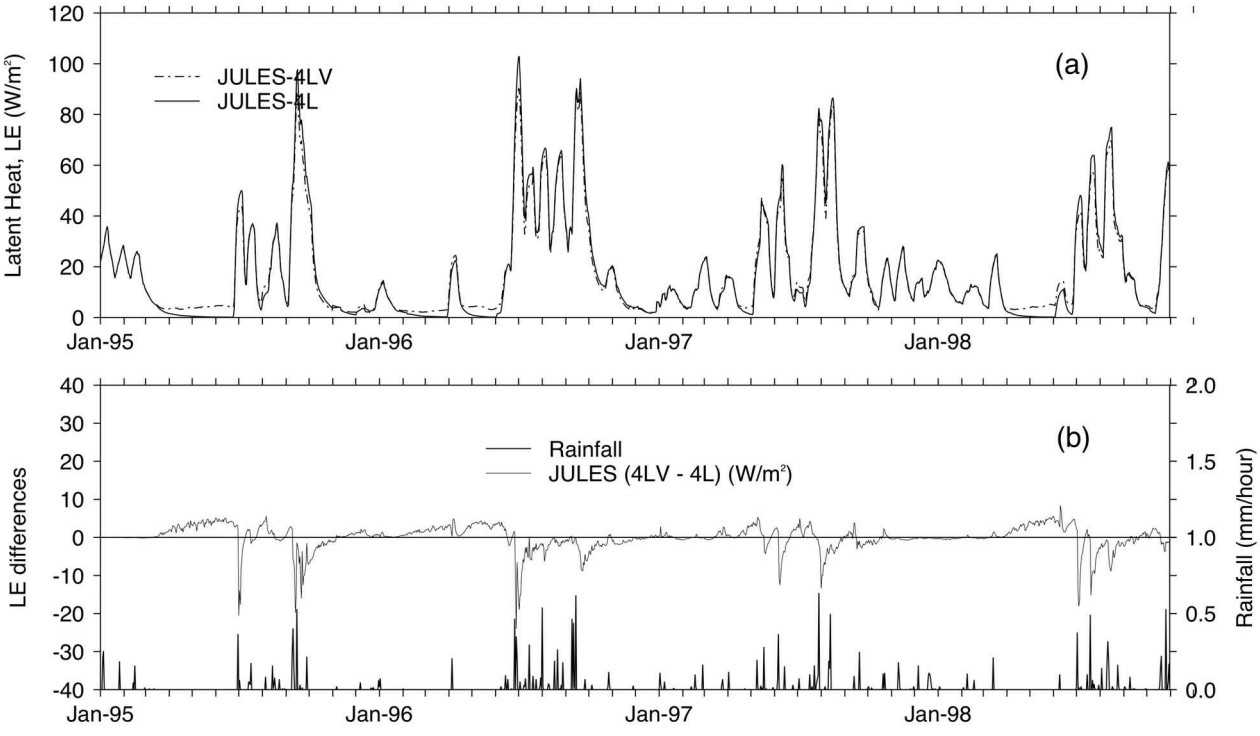

Figure 6. Modeled (a) latent heat flux (10 days moving average) (W m^{-2}) and (b) absolute [4LV-4L] daily difference of latent heat flux (in W m^{-2}) between modeled 4L and 4LV run for the Jornada site between 1995 and 1998. Rainfall events are also shown. The horizontal line was included to clearly distinguish between positive and negative latent heat flux differences.

of the topsoil layers. The influence that water vapor fluxes have on the water and heat transfer varies generally within years due to the local climatology.

[59] During the summer, for a period of no rain (between April and June), the 4LV model configuration tends to produce larger values of latent heat flux compared to the 4L run; during this period the 4L evaporation rates are very near zero, whereas 4LV predicts a more plausible, albeit low, evaporation rate, even when rainfall is absent. This pattern changes every summer during the rainy period, around June approximately (but a similar effect is observed early April 1996) when the latent heat is suppressed by up to 20 W m^{-2} for the 4LV run. The incorporation of water vapor flux has modified the water transfer between the soil layers (see Figures 1a and 2b) due to the activation of the isothermal and thermal vapor fluxes. Our results suggest that water vapor fluxes are able to significantly modify the surface energy balance via their effect on the water balance of the topsoil layers.

[60] Figure 7 shows measured and modeled (4L and 4LV) surface temperature and absolute differences between the 4LV and 4L runs for the Jornada site: absolute differences were between −0.5 and 0.5°C. Surface temperatures decrease when latent heat flux was enhanced (see Figure 7b), while they increase when the latent heat was suppressed. Soil moisture memory and the local precipitation patterns play an important role in the observed water transfer dynamics and evaporation rates. Overall, JULES-4LV showed an increased r^2 value of 0.89 when comparing between model estimates of surface temperature and measurements (0.86 for the 4L run), and a root mean square error of 3.9 (4.5 for the 4L run).

[61] Figure 8 presents modeled (4L and 4LV) latent heat flux for the long-term runs (between 2002 and 2007) performed for the Griffith site. Figure 9 shows modeled (4L and 4LV) surface temperature and absolute differences between the 4L and 4LV runs for the Griffith site. Differences between the standard JULES and the version considering water vapor flux were larger at this site, with differences of latent heat up to 35 W m^{-2} and differences of surface temperature between −3.0 and 1.0°C due to larger isothermal vapor fluxes observed at this site, as discussed in section 3.2. Unfortunately, neither measurements of latent heat nor surface temperature were available for the Griffith site.

[62] Figure 10 presents measured and modeled (4L and 4LV) latent heat flux for the long-term runs (between 2003 and 2005) performed for the Audubon site. Overall, JULES-4LV achieved a better model performance for the latent heat flux with a correlation coefficient of 0.78 for the 4LV run (0.58 for the 4L run) and a root mean square error of 29.25 (34.05 for the 4L run). JULES-4L tends to underestimate latent heat flux during the rainfall events that start each year by July (the onset of the rainy season), while JULES-4LV seems to capture more accurately the enhanced latent heat flux observed with absolute differences up to 80 W m^{-2}. JULES-4LV also better predicts the reduction of evaporation rates observed during the yearly drying out periods (up to 40 W m^{-2} reduction). The sign of change follows a course that is similar to those observed

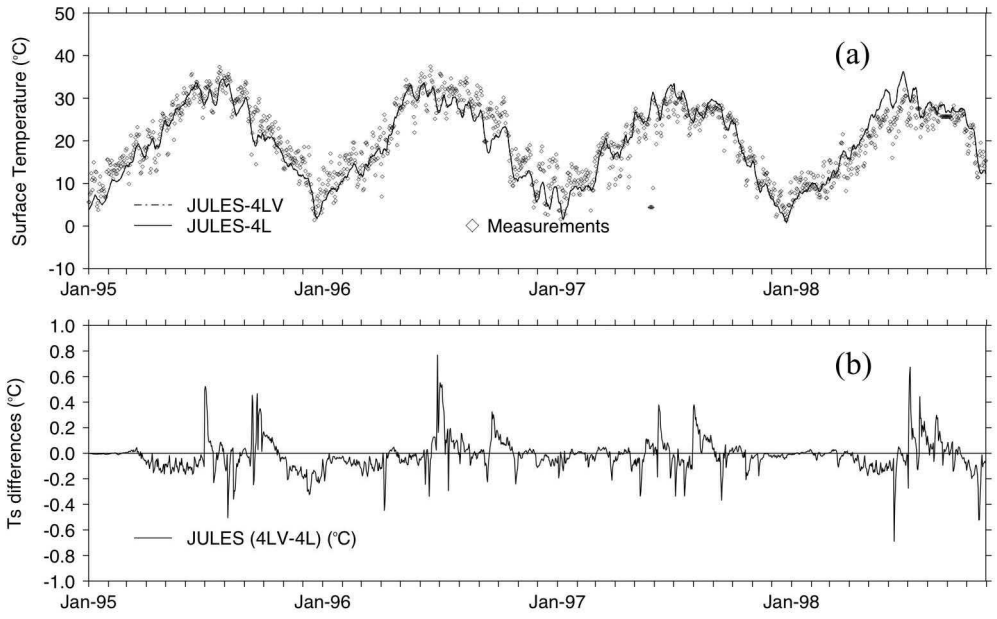

Figure 7. Measured and modeled (10 days moving average) (a) surface temperature (°C) and (b) absolute [4LV-4L] daily difference of surface temperature (in °C) between modeled 4L and 4LV run for the Jornada site between 1995 and 1998. The horizontal line was included to clearly distinguish between positive and negative temperature differences.

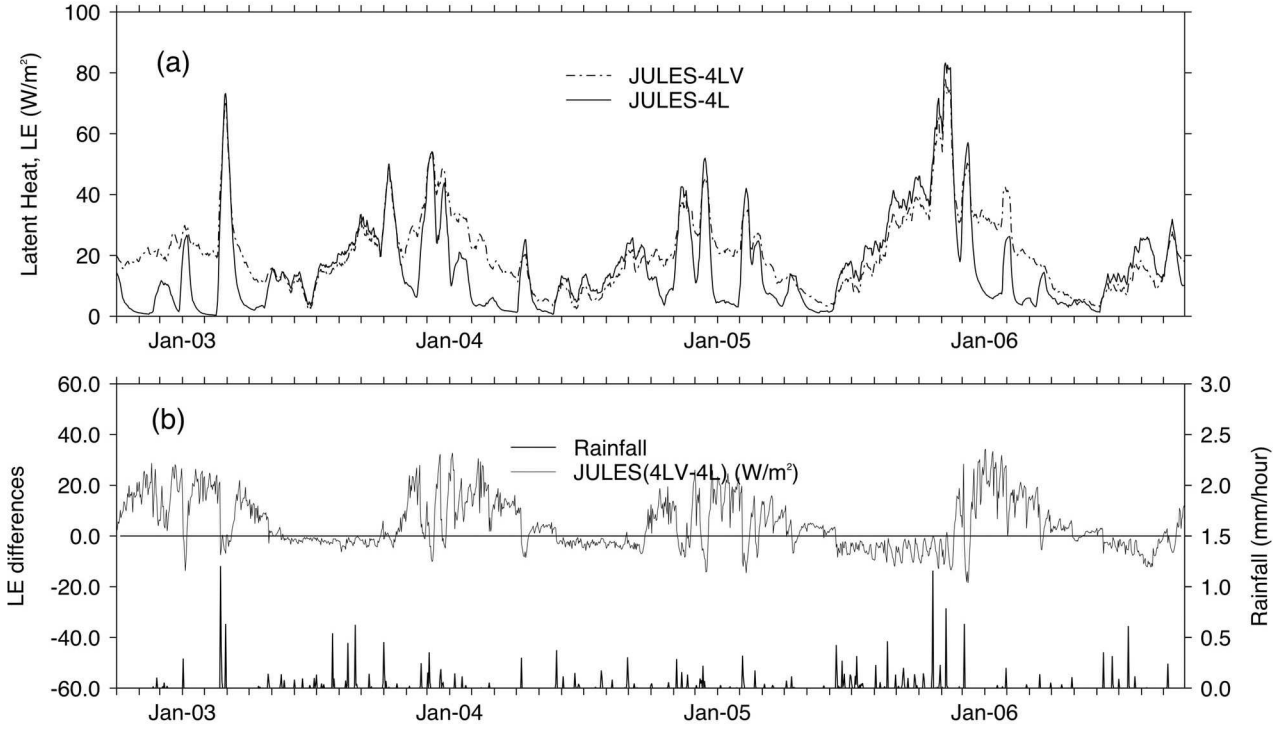

Figure 8. Modeled (a) latent heat flux (10 days moving average) (W m^{-2}) and (b) absolute [4LV-4L] daily difference of latent heat flux (in W m^{-2}) between modeled 4L and 4LV run for the Griffith site between 2002 and 2007. Rainfall events are also shown.

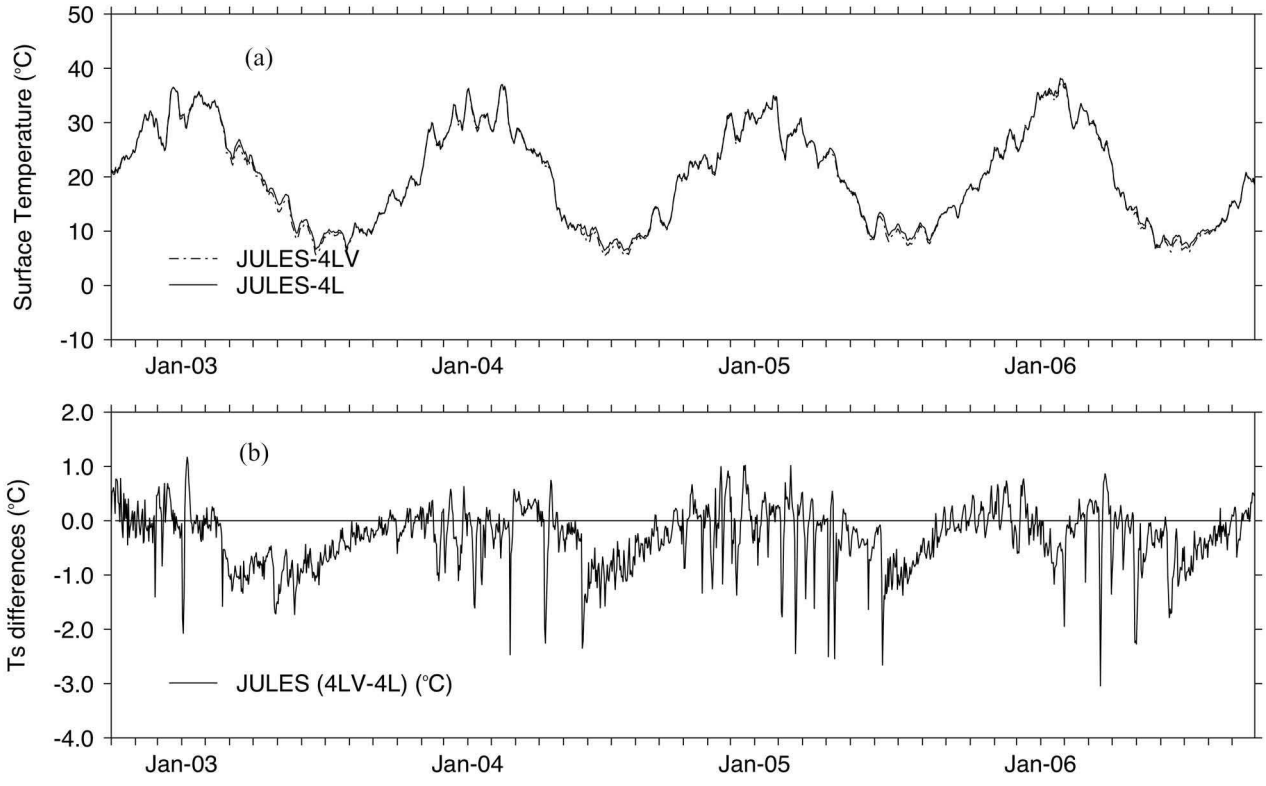

Figure 9. Modeled (a) surface temperature 10 days moving average (°C) and (b) absolute [4LV-4L] daily difference of surface temperature (in °C) between modeled 4L and 4LV run for the Griffith site between 2002 and 2007.

for the Jornada and Griffith site, although the magnitude is different due to different soil properties and different rainfall patterns that characterized each site.

[63] Figure 11 shows modeled (4L and 4LV) surface temperature and absolute differences between the 4L and 4LV runs for the Audubon site. Differences of surface temperatures between the standard JULES and the version considering water vapor flux were from −3.0 up to 2.0°C. These differences are larger than for the Jornada site and of the same order of magnitude as for the Griffith site.

[64] In summary, the incorporation of water vapor flux in the JULES LSM enhances latent heat flux, while surface temperature decreased, when it rains; during the dry down periods, latent heat flux is decreased instead, and surface temperatures tend to go up. During long dry periods, JULES-4LV seems to give larger values of latent heat compared to the standard JULES. Rainfall intensity and frequency would change slightly these general patterns within the sites.

[65] Generally, JULES has been found to overestimate the evaporation rates. These and other JULES deficiencies were discussed by *Blyth et al.* [2010] who used driving and verification data for sites with a wide range of climatic conditions and vegetation/soil types. Blyth et al. observed differences in seasonal variations of latent heat and CO_2 fluxes between JULES output and observations, in particular for dry land surfaces, which the authors suggested could be related to the soil hydraulic theory employed in JULES. Here we show that some of these discrepancies could have been caused by the fact that vapor fluxes have not been considered, until now.

3.4. Model Sensitivity of Vertical Soil Resolution

[66] We also explored the impact of the model's vertical soil resolution on the simulation of within-soil physical processes. In our study we tried to reach a compromise between numerical and process-simulation aspects. Operational models usually have a limited vertical soil resolution; in JULES it is constrained to four layers for regional and global simulations, although it is more flexible, in theory, for l-D simulations.

[67] *Best et al.* [2005] developed a scheme to calculate the optimal layer thicknesses for the JULES model, using a Monte Carlo method. We performed a sensitivity test, using JULES with the water vapor flux incorporated, with six instead of four layers. Optimized layer thicknesses were 0.03, 0.03, 0.16, 0.45, 1.0, and 1.87 m, respectively; i.e., a higher vertical resolution for the first three layers compared to the standard JULES. Note that JULES becomes unstable if the top layer is less than 0.025 m thick (even if using a shorter time step), so we cannot reduce the soil layer thickness further.

[68] The simulation with the modified six layer model for the Griffith site indicated that increasing the vertical soil resolution near the surface did not change the seasonal course of soil moisture content. Differences in evaporation between the JULES-4LV and JULES-6LV run were up to 5 W m^{-2}. We recognize that sensitivity to vertical soil

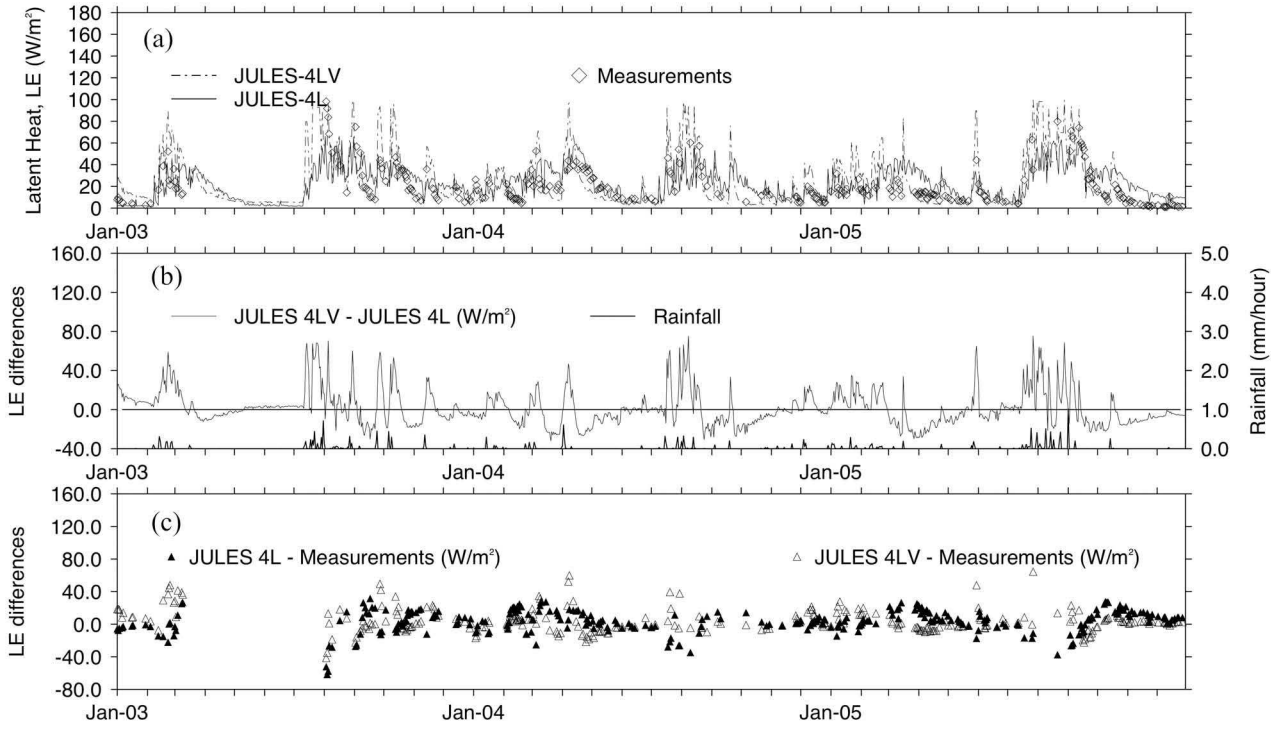

Figure 10. Measured and modeled (a) latent heat flux (10 days moving average) (W m^{-2}); (b) absolute [4LV-4L] daily difference of latent heat flux (in W m^{-2}) between modeled 4L and 4LV run for the Audubon site between 2003 and 2005; and (c) absolute daily differences of latent heat flux (in W m^{-2}) between modeled 4L/4LV and measurements. Rainfall events are also shown. Latent heat flux measurements are also included (diamonds).

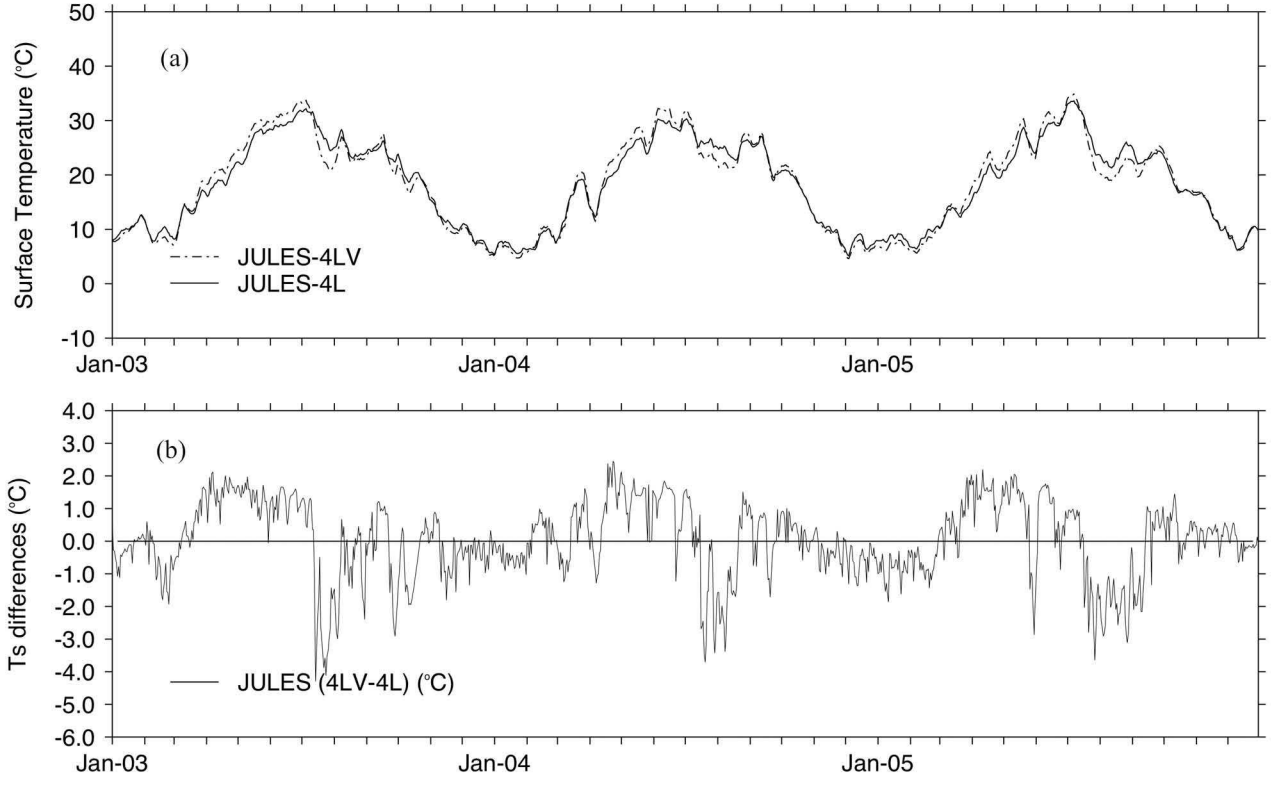

Figure 11. Modeled (a) surface temperature 10 days moving average (°C) and (b) absolute [4LV-4L] daily difference of surface temperature (in °C) between modeled 4L and 4LV run for the Audubon site between 2003 and 2005.

resolution is a significant factor that should be explored in further studies.

4. Conclusions

[69] The focus of this study concerns the mechanisms behind the water and heat transfer in upper soil layers and their consequences in terms of the energy balance. The simplified Richards equation, still widely used in most LSMs, has been updated in the JULES LSM by incorporating water vapor transfer; the effect of this new configuration was tested for three sites. For these (semi-)arid locations, inclusion of water vapor transfer appears to have improved predicted seasonal courses of soil moisture profiles and latent heat flux. The combined isothermal and thermal vapor fluxes plays a relatively important role, significantly modifying the energy and water balance of the topsoil layers which could have an impact on the hydrology of not only semiarid environments but also under midlatitude climatic conditions, where soil moisture content and groundwater levels display strong intraseasonal variability and are likely to decrease in the next decades. The effect of the inclusion of water vapor flux also introduced a different diurnal evolution in the latent heat, soil moisture content, and surface temperature.

[70] These off-line simulations have been a valuable tool to evaluate the JULES land surface scheme; however, coupled land-atmosphere simulations at the mesoscale will allow us to evaluate JULES's performance, and understand the impact of the improved water transfer in the upper soil layers, on a global scale. After these simulations we would be in a better position to recommend the incorporation of water vapor flux in other land surface and operational models. Increased vertical resolution in the soil will also be needed to better characterize the development of the drying front during the different evaporation stages and soil moisture memory [*Seneviratne et al.*, 2006]. These improvements could potentially increase the coupling strength between the soil-vegetation and the lower atmosphere, which could have important implications for climate and weather predictions [see for example, *Koster et al.*, 2004].

[71] **Acknowledgments.** This work was supported by the UK Natural Environment Research Council (NERC) (GROund coupled heat pumps MITigation potential, NE/F020368/1). The Jornada data sets were provided by the Jornada Long-Term Ecological Research (LTER) project by the U.S. National Science Foundation (grant DEB-0080412). The Griffith data were provided by NCAR/EOL under sponsorship of the National Science Foundation (Murrumbidgee Surface Meteorology and Radiation Data Set). The authors also thank the AmeriFlux principle investigator, Tilden P. Meyers for access to Audubon Ranch data. We are grateful to Tony Scott (Rothamsted Research, Harpenden, UK) for providing hourly meteorological data from the Rothamsted Automatic Weather Station and from the Environmental Change Network (ECN) Automatic Weather Station.

References

Best, M. J., P. Cox, and D. Warrilow (2005), Determining the optimal soil temperature scheme for atmospheric modeling applications, *Bound-Lay Meteorol*, *114*, 111–142.

Best, M. J., et al. (2011), The Joint UK Land Environment Simulator (JULES), model description—Part 1: Energy and water fluxes, *Geosci. Model Dev.*, *4*, 677–699, doi:10.5194/gmd-4-677-2011.

Bittelli, M., F. Ventura, G. S. Campbell, R. Snyder, F. Gallegati, and P. Pisa (2008), Coupling of heat, water vapor, and liquid water fluxes to compute evaporation in bare soils, *J. Hydrol.*, *362*, 191–205.

Blyth, E., J. Gash, A. Lloyd, M. Prior, G. Weedon, and J. Shuttleworth (2010), Evaluating the JULES land surface model energy fluxes using fluxnet data, *Am. Meteorol. Soc.*, *11*, 509–519.

Braud, I., A. Dantas-Antonino, M. Vauclin, J. Thony, and P. Ruelle (1995), A simple soil-plant-atmosphere transfer model (SISPAT) development and field verification, *J. Hydrol.*, *166*, 213–250.

Braud, I., T. Bariac, P. Biron, and M. Vauclin (2009), Isotopic composition of bare soil evaporated water vapor. Part II: Modeling of rubic IV experimental results, *J. Hydrol.*, *369*, 17–29.

Brooks, R. H., and A. T. Corey (1964), *Hydraulic properties of porous media*, pp. 620–634, Paper 3, Colorado State University, Fort Collins, Colorado.

Calvet, J. C., J. Noilhan, and P. Bessemoulin (1998), Retrieving the root-zone soil moisture from surface soil moisture or temperature estimates: A feasibility study based on field measurements, *Am. Meteorol. Soc.*, *37*, 371–386.

Cass, A., G. S. Campbell, and T. L. Jones (1984), Enhancement of thermal water vapor diffusion in soil, *Soil Sci. Soc. Am. J.*, *48*(1), 25–32.

Celia, M. A., E. T. Bouloutas, and R. L. Zarba (1990), A general mass-conservative numerical solution for the unsaturated flow equation, *Water Resour. Res.*, *26*(7), 1483–1496.

Clark, D. B., et al. (2011), The Joint UK Land Environment Simulator (JULES), model description—Part 2: Carbon fluxes and vegetation dynamics, *Geosci. Model Dev.*, *4*, 701–722, doi:10.5194/gmd-4-701-2011.

Cosby, B. J., G. M. Hornberger, R. B. Clapp, and T. R. Ginn (1984), A statistical exploration of the relationships of soil moisture characteristics to the physical properties of soils, *Water Resour. Res.*, *20*(6), 682–690.

Cox, P., C. Huntingford, and R. J. Harding (1998), A canopy conductance and photosynthesis model for use in a GCM land surface scheme, *J. Hydrol.*, *212–213*, 79–94.

Cox, P., R. Betts, C. Bunton, R. Essery, P. Rowntree, and J. Smith (1999), The impact of new land surface physics on the GCM simulation of climate and climate sensitivity, *Clim. Dyn.*, *15*, 183–203.

Egea, G., A. Verhoef and P. L. Vidale (2011), Towards an improved and more flexible representation of water stress in coupled photosynthesis–stomatal conductance models, *Agric. For. Meteorol.*, *151*(10), 1370–1384.

Gran, M., J. Carrera, S. Olivella and M. W. Saaltink (2011), Modelling evaporation processes in a saline soil from saturation to oven dry conditions, *Hydrol. Earth Syst. Sci. Discuss*, *8*, 529–554.

Grifoll, J., J. Gasto, and Y. Cohen (2005), Non-isothermal soil water transport and evaporation, *Adv. Water Resour.*, *28*, 1254–1266.

Ho, C. K., and S. W. Webb (1999), Enhanced vapor-phase diffusion in porous media-LDRD final report, Sandia National Laboratories, Albuquerque, NM.

Jung, M., G. Le Maire, S. Zaehle, S. Luyssaert, M. Vetter, G. Churkina, P. Ciais, N. Viovy, and M. Reichstein (2007), Assessing the ability of three land ecosystem models to simulate gross carbon uptake of forests from boreal to Mediterranean climate in Europe, *Biogeosciences*, *4*(4), 647–656.

Kimball, B. A., R. D. Jackson, R. J. Reginato, F. S. Nakayama, and S. B. Idso (1976), Comparison of field-measured and calculated soil heat fluxes, *Soil Sci. Soc. Am. Proc.*, *40*(1), 18–25.

Koster, R. D., and M. J. Suarez (2001), Soil moisture memory in climate models, *J. Hydrometeorol.*, *2*(6), 558–570.

Koster, R. D., et al. (2004), Regions of strong coupling between soil moisture and precipitation, *Science*, *305*(5687), 1138–1140.

Lai, S., J. M. Tiedje, and A. E. Erickson (1976), In situ measurement of gas diffusion coefficients in soils, *Soil Sci. Soc. Am. Proc.*, *40*(1), 3–6.

Lee, D. H. and L. Abriola (1999), Use of Richards equation in land surface parameterizations, *J. Geophys. Res.*, *104*, 27,519–27,526.

Lu, S., T. Ren, Y. Gong, and R. Horton (2007), An improved model for predicting soil thermal conductivity from water content at room temperature, *Soil Sci. Soc. Am. J.*, *71*, 8–14.

Lu, S., T. Ren, Z. Yu, and R. Horton (2011), A method to estimate the water vapour enhancement factor in soil, *Eur. J. Soil Sci.*, *62*, 498–504.

Meyers, T. (2009), Audubon Research Ranch FLUXNET L3 and L4 Data, ftp://cdiac.ornl.gov/pub/ameriflux/data/Level4/Sites_ByName/Audubon_Grasslands/, Carbon Dioxide Inf. Anal. Cent., Oak Ridge Natl. Lab., Oak Ridge, TN.

Milly, P. (1982), Moisture and heat transport in hysteretic inhomogeneous porous media: A matric head-based formulation and a numerical model, *Water Resour. Res.*, *18*, 489–498.

Milly, P. (1984), A simulation analysis of thermal effects on evaporation from soil, *Water Resour. Res.*, *20*, 1087–1098.

Nash, M. H., and L. A. Daugherty (1990), Soil-landscape relationships in alluvium sediments in Southern New Mexico, Agricultural Experiment Station, *Bulletin 746*, College of Agriculture and Home Economics, New Mexico State University.

Philip, J. R. and V. D. De Vries (1957), Moisture movement in porous materials under temperature gradient, *Trans. Am. Geophys. Union*, *38*(2), 222–232.

Richter, H., A. W. Western, and F. H. S. Chiew (2004), The effect of soil and vegetation parameters in the ECMWF Land Surface Scheme, *Am. Meteorol. Soc.*, *5*, 1131–1146.

Saito, H., J. Simunek, and B. Mohanty (2006), Numerical analysis of coupled water, vapor and heat transport in the vadose zone, *Vadose Zone J.*, *5*, 784–800.

Saravanapavan, T., and G. D. Salvucci (2000), Analysis of rate-limiting processes in soil evaporation with implications for soil resistance models, *Adv. Water Resour.*, *23*, 493–502.

Scanlon, B. R. and P. C. D. Milly (1994), Water and heat fluxes in desert soils. Numerical simulations, *Water Resour. Res.*, *3*(3), 721–733.

Seneviratne, S. I., et al. (2006), Soil moisture memory in AGCM simulations: Analysis of global land-atmosphere coupling experiment (GLACE) data, *J Hydrometeorol.*, *7*(5), 1090–1112.

Shahraeeni, E., and D. Or (2010),. Thermo-evaporative fluxes from heterogeneous porous surfaces resolved by infrared thermography, *Water Resour. Res.*, *46*, W09511, doi:10.1029/2009WR008455.

Shokri, N., P. Lehmann, and D. Or (2009), Critical evaluation of enhancement factors for vapor transport through unsaturated porous media, *Water Resour. Res.*, *45*, W10433, doi:10.1029/2009WR007769.

Stockli, R., P. Vidale, A. Boone, and C. Schär (2007), Impact of scale and aggregation on the terrestrial water exchange: Integrating land surface models and Rhone catchment observations, *J. Hydrometeorol.*, *8*, 1002–1015.

Ten Berge, H. (1990), *Heat and Water Transfer in Bare Topsoil and the Lower Atmosphere, 33*, 207 pp., Simulation Monographs, Pudoc, Wageningen, The Netherlands.

Teuling, A. J., R. Uijlenhoet, F. Hupet, and P. A. Troch (2006), Impact of plant water uptake strategy on soil moisture and evapotranspiration dynamics during drydown, *Geophys. Res. Lett.*, *33*, L03401, doi:10.1029/2005GL025019.

Thompson, S. E., C. J. Harman, A. G. Konings, M. Sivapalan, A. Neal, and P. A. Troch (2011), Comparative hydrology across AmeriFlux sites: The variable roles of climate, vegetation, and groundwater, *Water Resour. Res.*, *47*, W00J07, doi:10.1029/2010WR009797.

Varado, N., I. Braud, P. Ross, and R. Haverkamp (2006), Assessment of an efficient numerical solution of the 1D Richards' equation on bare soil, *J. Hydrol.*, *323*, 244–257.

Wondzell, S. M., J. M. Cornelius, and G. L. Cunningham (1990), Vegetation patterns, microtopography, and soils on a Chihuahuan desert playa, *J. Vegetation Sci.*, *1*, 403–410.

Young, R., J. Walker, N. Yeoh, A. Smith, K. Ellett, O. Merlin, and A. Western (2008), *Soil moisture and meteorological observations from the Murrumbidgee catchment, technical report*, Dep. of Civil and Environ. Engin., Univ. of Melbourne, Melbourne, VIC, Australia.

Zaehle, S., P. Friedlingstein, and A. D. Friend (2010a), Terrestrial nitrogen feedbacks may accelerate future climate change, *Geophys. Res. Lett.*, *37*, L01401, doi:10.1029/2009GL041345.

Zaehle, S., A. D. Friend, P. Friedlingstein, F. Dentener, P. Peylin, and M. Schulz (2010b), Carbon and nitrogen cycle dynamics in the O-CN land surface model: 2. Role of the nitrogen cycle in the historical terrestrial carbon balance, *Global Biogeochem. Cycles*, *24*, GB1006, doi:10.1029/2009GB003522.

I. Braud, Unité de recherche Hydrologie-Hydraulique, IRSTEA, 3 bis quai Chauveau, CP 220, F-69336 Lyon CEDEX 9, France.

R. Garcia Gonzalez and A. Verhoef, Department of Geography and Environmental Science, School of Human and Environmental Sciences, Whiteknights Campus, University of Reading, PO Box 227, Reading RG6 6DW, United Kingdom. (r.garciagonzalez@reading.ac.uk; rgarciagonzalez1@gmail.com)

P. Luigi Vidale, NCAS-Climate, Meteorology Bldg., Whiteknights Campus, University of Reading, PO Box 243, Reading RG6 6BB, United Kingdom.